



ANALYTICAL INVESTIGATION OF FIVE ROMAN Pb-BASED SCALE WEIGHTS (QASR AR-RABBAH, JORDAN): A CASE STUDY

**Ahmad Abu-Baker¹, Wassef Al Sekhaneh^{1,2*}, Atef Shiyab¹, Jan Dellith²,
Andy Scheffel², M. Anwar Alebrahim², Jürgen Popp^{2,3}**

¹*Faculty of Archaeology and Anthropology-Conservation of Cultural Resources-Applied Science
in archaeology, Yarmouk University, Postal code 211-63, Irbid, Jordan*

²*Institute of Photonic Technology, Albert-Einstein-Str. 9, 07745 Jena, Germany*

³*Institute of Physical Chemistry and Abbe Center of Photonics, University Jena, Helmholtzweg 4, 07743
Jena, Germany*

Received: 20/03/2013

Accepted: 25/04/2013

Corresponding author: sekhaneh@yahoo.de

ABSTRACT

The composition and corrosion behavior of five archaeological lead scale weights from Qasr Ar-Rabbah in Jordan is studied using scanning electron microscopy with energy dispersive X-ray micro-analysis (SEM-EDX). X-ray diffraction (XRD) analysis was used to identify the mineralogical composition of the corrosion layers. It is found that the weights were relatively pure lead objects with the presence of minor elements that were associated with lead in its ores. The corrosion layers were basically composed of the stable corrosion product cerussite PbCO_3 , which however obscured the surface details and contained micro-cracks.

KEYWORDS: Roman, Lead, corrosion, lead scale weight, SEM-EDX, XRD

1. INTRODUCTION

Lead was one of the earliest metals discovered and extracted from its ores (Craddock, 1995). The Roman period witnessed an increase in the use and applications of the metal (Woolley, 1984; Retief and Cilliers, 2006). Among the various uses of lead was its use in making weights for trade and coinage. Being available in the Roman Empire, easy to extract from its ores, with a low melting-point and easy to cast into molds, relatively inert in air, and dense metal made lead very useful for this use (Pulsifer, 1888; Nriagu, 1983).

Most of previous studies on archaeological lead weights were only stylistic and descriptive (Hultsch, 1882; Lang and Crosby, 1964; Meyer and Moreno, 2004). Exploring previous investigations of other soil-buried archaeological lead artifacts shows that they usually develop insoluble layers of lead corrosion products by the reaction of lead ions with the soil dissolved anions. The result of the corrosion process is a thin insoluble film of lead (II) oxide (PbO) covered with a corrosion layer of insoluble lead salts such as cerussite (PbCO₃) and hydrocerussite (Pb₃(OH)₂(CO₃)₂) in calcareous soil. Depending on the soil conditions and type of anions present, lead chlorides and sulfates may also form (Carradice and Campbell, 1994; Selwyn 2004; Alhassan, 2005). As can be drawn from the equilibrium potential-pH diagram of lead-water system, the lead (IV) compounds such as lead (IV) oxide (PbO₂) only occur in intensely oxidizing atmospheres, and that is why they are less detected in the corrosion products of lead artifacts (Caley, 1955; Turgoose, 1985).

The above mentioned corrosion products are stable and protective for the metal, however a long exposure to the corrosive anions will accelerate the corrosion process, which will decrease the cohesion and ductility and obscure the surface details of the artifact (Mattias *et al.*, 1984). The worst consequence happens if the environment of lead artifact contains a vapor or solution of organic acids such as acetic acid and formic acid. These acids react with lead and form soluble lead

acetate and formate. The diffused lead ions of these corrosion products will then react with moisture and carbon dioxide to form an un-protective powdery basic lead carbonate, and the acetate and formate ions will continue to cause further lead to corrode (lead disease). (Mattias *et al.*, 1984; Cronyn, 1990; Selwyn, 2004; Bernard *et al.*, 2009).

As the selection of suitable conservation treatment of lead-based artifacts requires the determination of the composition and nature of the original material and corroded surface (Costa and Urban, 2005), this study aimed to investigate the corrosion and elemental composition of five lead scale weights from Qasr Ar-Rabbah as a sample of small lead artifacts from the Roman period in Jordan. Mineralogical and elemental analyses of the corrosion products were used to explain the state of preservation of the artifacts, and the environmental conditions of the burial soil in the archaeological site. Scanning electron microscopy combined with energy dispersive X-ray micro analysis of cross-sections taken from the artifacts was used to examine the extent of the corrosion layer and the elemental composition of the un-corroded internal metal/alloy. The results of these examinations were essential to explain technical aspects of the production of Roman lead weights, and to determine the suitable treatment for these artifacts.

2. THE SITE

The excavation works were carried out at the archaeological site of Qasr Ar-Rabbah (Al Qasr) which is located in the mid-west of Jordan, 5 km from Ar-Rababah which lies approximately 15 km north of Al-Karak city (Fig.1). Al-Shiyab (1993) undertook a thorough archaeological study in the Qasr Ar-Rabba site.

The construction style of the tombs that were found at the site resembles those included within Type-I style tombs identified at Hesban region in Jordan, which is chronologically attributed to the late Hellenistic to Late Roman periods (Waterhouse, 1998). The configuration of the tomb structure was found to include loculi that radiate from a central chamber, and benches along the walls

of the chamber. Based on these architectural characteristics and relative dating of a large quantity of ceramics recovered from the graves at site, the site was dated to the Late Roman period (Al-Shiyab, 2002). The samples were found in the same layer of the tombs therefore, the lead weight samples investigated in this study can be dated to this period.

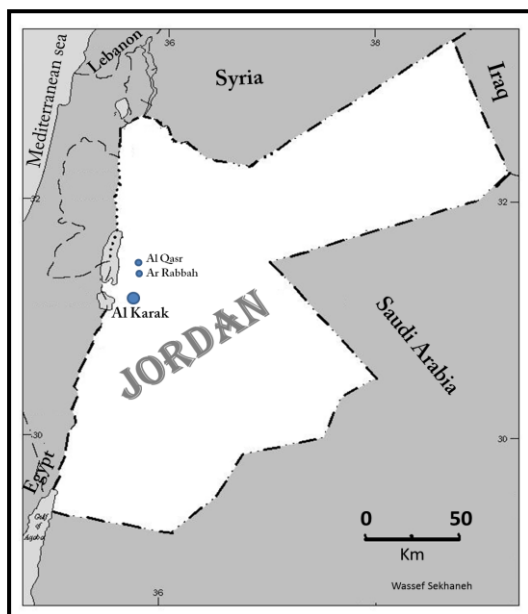


Fig. 1: Location map of Qasr Ar-Rabbah archaeological site in Jordan

3. THE ARTIFACTS

Five lead-based scale weights excavated from Qasr Ar-Rabba archaeological site are investigated in this study. Figure 2 shows the

archaeological remains in which the lead weight samples were found.



Figure 2: View of archaeological remains excavated at Qasr Ar-Rabbah in which the lead-based scale-weights were found (white circle).

Table 1 shows images of the artifacts, their weights and dimensions. Preliminary visual and microscopic examinations of the artifacts show that their originally grey surfaces are almost covered with soil deposits, substantial uniform whitish corrosion layers that hide the original surfaces' details. No powdery active corrosion spots were detected on the surface of the artifacts; however some parts of the outer surfaces have small cracks. In general, the artifacts could be considered in a good condition with no major missing parts or fragile surfaces; however the inscriptions are obscured by the corrosion products and surface incrustations.

Table 1: Images, weights and dimensions of the lead-based weights		
1. Oval lead weight		Weight: 37.16g Length: 30.60mm Max. width: 19.70mm Max. thickness: 11.40mm
2. Square lead weight		Weight: 27.58g Length: 26.91mm Width: 26.45mm Thickness: 4.28mm

3. Perforated square lead weight		Weight: 6.62g Length: 16.98mm Width: 16.27mm Thickness: 3.24mm
4. Cubic lead weight		Weight: 11.68g Cubic: 10.93x10.88x10.44mm
5. Cylindrical lead weight		Weight: 5.34g Length: 11.16mm Width: 9.74mm Thickness: 6.29mm

4. THE ROMAN WEIGHT SYSTEM

The Romans had a duodecimal weight system. The *Libra* was the weight for the Roman pound. The smallest part of the twelve parts of *Libra* was the *Uncia* or Roman ounce. The *Uncia* also had subdivision weights that were based on the factor of 12. In today's metric system of weight (technically mass), the *Libra* approximately equals 327.45 g and the *Uncia* approximately equals 27.29 g (Hultsch, 1882; Lang and Crosby, 1964).

The measured weights of the artifacts investigated in this study could be used to identify their Roman names. However, one should notice that the weights have corroded over the years, and that they may have small missing parts or surface deposits, which may slightly decrease or increase the weight, respectively. With these considerations into, a preliminary identification based on weight is presented here, and future conservation work on the artifacts will hopefully reveal the surface details

currently obscured by the corrosion layer, which will add further evidence on the identity of these artifacts.

The weight no. 1, the oval lead weight, weighs 37.16g, which is about 4g less than the weight of the Roman Sescuncia or 1/8 *Libra*, and this can be attributed to the fact that the object has small missing parts as a result of corrosion. The weight no. 2, the square lead weight, weighs 27.58g, which almost equals the weight of the Roman *Uncia* (ounce). The weight no. 3, the perforated square lead weight, weighs 6.62g which is very close to the weight of Roman *Sicilicius* or 1/4 *Uncia*. The weight no. 4, the Cubic lead weight, weighs 11.68g which is about 2g less than the weight of the Roman *Semuncia* or 1/2 *Uncia*, and this can be attributed to losing some weak corroded parts from the artifact. The last artifact, the weight no. 5, the cylindrical lead weight, weighs 5.34g, which is close to the weight of Roman *Sextula* or 1/4 *Uncia* (Cagnat, 1898).

5. EXPERIMENTAL PROCEDURE

The corrosion products were investigated and characterized by X-ray diffraction (XRD), field emission scanning electron microscopy (FE-SEM) combined with energy dispersive X-ray spectrometry (EDX).

The mineralogical composition of the corrosion products was determined using a Shimadzu LabX, XRD-6000 X-ray diffractometer. A small amount of the corrosion products was scratched off of the surface of each artifact, then mixed and dispersed in ethanol and spread on a microscopic glass slide. After the evaporation of ethanol, the slide was brought into the XRD instrument for analysis. Copper $KL_{2,3}$ ($\alpha_{1,2}$) radiation ($\lambda=1.5418\text{\AA}$) was used for the analysis and the spectrum was acquired at 40 kV, 30 mA and a step size of 0.05° in 2θ . The assignment of the minerals was based on the database of the Joint Committee Powder Diffraction Standards-International Centre for Diffraction Data (JCPDS-ICDD).

SEM combined with EDX was used to examine the elemental composition of the corrosion products and original material. This technique was used in order to obtain further information about the nature of the minor or amorphous corrosion products that would have not appeared in the XRD spectrum. Cross-sections were taken from the edge of each artifact using a fine jeweller's saw. The five objects were photographically documented before and after taking the cross-sections. The cross-sections were embedded in an Araldite 2020 epoxy resin. Following curing for 24 hours, the samples were ground on a series of silicon carbide papers from 150 to 1200 grit and then polished on a Buehler minimet polisher beginning at 9–3 μm alumina polishing suspensions and reducing down to a highly polished surface using 1–0.25 μm diamond pastes. The samples were then decontaminated in ethanol in an ultrasonic bath and finally dried. The SEM/EDX investigation was carried out using a high resolution field emission electron microscope JSM-6300 F combined with a microprobe analyzer JXA-8800 L (JEOL, Japan). The SEM micrographs were taken

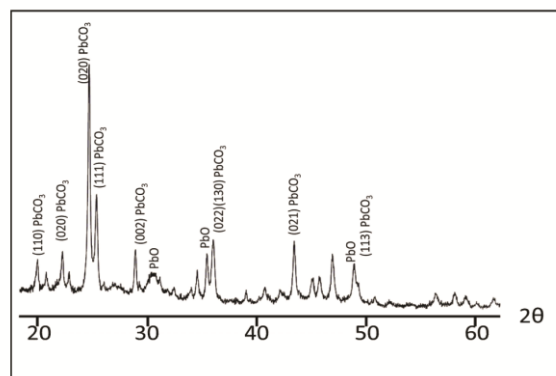
using the ordinary secondary electron (SE) mode that is more often used to show the morphology and topography of the sample, then using back-scattered electron (BSE) mode in order to obtain a compositional contrast and in this manner a first analytical information. Here, a more bright contrast indicates a region of higher medium atomic number containing more heavy elements. In contrast, a tendentially dark appearing area consists of lighter elements. The energy dispersive X-ray spectrometry was used for the qualitative elemental identification. To this end a silicon drift detector (SDD) X-flash 5010 (BRUKER-Nano company, Germany) was used.

6. RESULTS AND DISCUSSION

6.1 X-RAY DIFFRACTION ANALYSIS

The XRD characterization of the corrosion products on the artifacts is shown in Fig. 3. The peaks in the diffractogram are in accordance with that of lead carbonate (cerussite PbCO_3) in the JCPDS-ICDD powder diffraction database and previous examinations reported in the literature (Brooker et al., 1983). The formation of this stable corrosion product is expected in the calcareous burial context of the artifacts (Mattias et al., 1984; Nosek, 1985).

Figure 3: XRD spectrum of the corrosion on the lead



weights with cerussite PbCO_3 being the main corrosion product.

It is always expected to detect cerussite (PbCO_3) or hydrocerussite ($\text{Pb}_3(\text{OH})_3(\text{CO}_3)_2$) in carbonated aqueous environment. The two compounds are in equilibrium at a carbon dioxide pressure of $10^{-2.8}$ atm as the following equation shows:



Therefore, hydrocerussite ($\text{Pb}_3(\text{OH})_3(\text{CO}_3)_2$) is the main corrosion product of lead artifacts exposed to the open atmosphere for a long time, because the atmospheric pressure of carbon dioxide (i.e. $10^{-3.5}$ atm) is less than that of equilibrium. While cerussite is the main corrosion product of lead artifacts buried in aerobic alkaline carbonated soil, where the carbon dioxide pressure is usually about 10^{-2} atm, and this is above the equilibrium value (Turgoose, 1985). This confirms the XRD analysis result for the lead weights.

6.2 SCANNING ELECTRON MICROSCOPY\ENERGY DISPERSIVE X-RAY MICRO ANALYSIS

The corrosion profile of the oval lead weight was investigated using SEM-EDX. The Backscattered Electron Emission (BSE) and SEM images show a cracked corrosion layer, with a thickness of about 100 microns, above the internal metal (Fig. 4). The EDX analysis shows that the corrosion layer (area-a in the SEM image) contains lead, calcium, oxygen, carbon, phosphorous and silicon. This suggests that the surface of the artifact is covered with lead carbonate (cerussite PbCO_3) that is mixed with calcium carbonate and siliceous soil deposits, which agrees with the XRD result. The presence of phosphorous in the corrosion layer could indicate the presence of pyromorphite $\text{Pb}_5\text{Cl}(\text{PO}_4)_3$. The EDX analysis of the internal material (area-b in the SEM image) shows that the artifact was cast from a relatively pure lead metal. No alloying elements were added to lead in the manufacture of this artifact. The presence of aluminium and silicon in the EDX analysis is expected because of the penetration of abrasive materials into the soft lead surface during the polishing of the cross-sections (Scott, 1996). The silicon carbide abrasive residues appear as black spots in the BSE mode SEM image, and as dark grey particles in the SE mode SEM image. The same situation can be seen in the rest of the cross-sections.

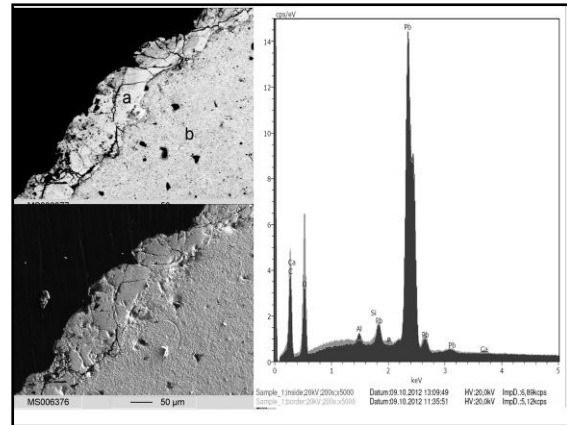


Figure 4: Backscattered (up) and secondary (down) electron SEM images of the oval lead weight and corresponding EDX elemental analysis of corrosion (light line) and internal metal (dark line)

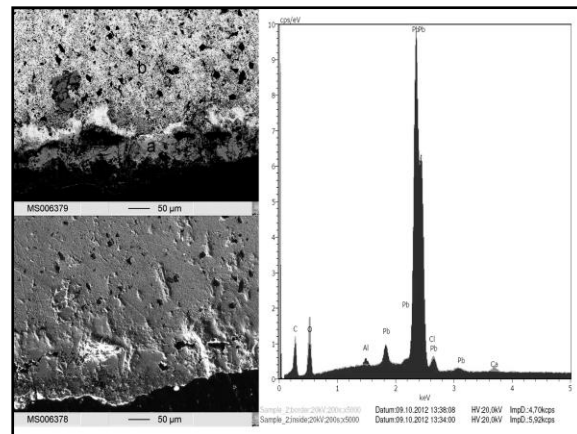


Figure 5: Backscattered (up) and secondary (down) electron SEM images of the the square lead weight and corresponding EDX elemental analysis of corrosion (light line) and internal metal (dark line)

Similarly, the BSE and SE images of the square lead weight show a cracked corrosion layer above the internal metal (Fig. 5). The EDX analysis shows that the corrosion layer (area-a in the SEM image) contains lead, calcium, oxygen, carbon and chlorine. This suggests that the surface of the artifact is covered with lead carbonate (cerussite PbCO_3) with the presence of lead chloride (cotunnite PbCl_2) and/or lead carbonate chloride (phosgenite $\text{Pb}_3\text{CO}_3\text{Cl}_2$) and/or lead chloride hydroxide (laurionite $\text{Pb}(\text{OH})\text{Cl}$) as secondary corrosion products, and calcium carbonate incrustations. The EDX analysis of the internal material (area-b in the SEM image) shows that the artifact was also cast from a relatively pure lead metal. No alloying elements were

added to lead in the manufacture of this artifact.

The BSE and SE images of the perforated square lead weight show a relatively thick corrosion layer (~250 micron) above the internal alloy (Fig. 6). The EDX analysis shows that the corrosion layer (area-a in the SEM image) contains lead, calcium, oxygen, carbon, chlorine and silicon. This suggests that the surface of the artifact is covered with lead carbonate (cerussite $PbCO_3$) as the principle constituent with the presence of lead chloride (cotunnite $PbCl_2$) and/or lead carbonate chloride (phosgenite $Pb_3CO_3Cl_2$) and/or lead chloride hydroxide (laurionite $Pb(OH)Cl$) as secondary corrosion products, and siliceous deposits. The EDX analysis of the internal material (area-b in the SEM image) shows that tin is present as a minor alloying element with lead.

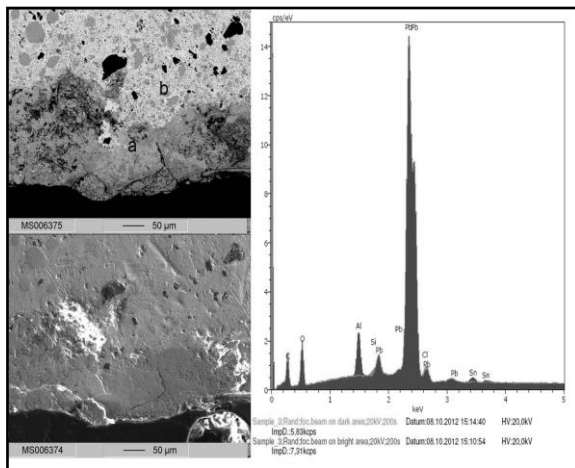


Figure 6: Backscattered (up) and secondary (down) electron SEM images of the the perforated square lead weight and corresponding EDX elemental analysis of Corrosion (light line) and internal metal (dark line)

The BSE and SEM images of the cubic lead weight show an irregular corrosion layer above the internal alloy (Fig. 7). The EDX analysis shows that the corrosion layer (area-a in the SEM image) contains lead, arsenic, antimony, oxygen, carbon, chlorine and silicon. From the elemental analysis which has been done by EDX we suggest that the surface of the artifact is covered with lead carbonate (cerussite $PbCO_3$) as

the principle constituent with the presence of lead chloride (cotunnite $PbCl_2$) and/or lead carbonate chloride (phosgenite $Pb_3CO_3Cl_2$) and/or lead chloride hydroxide (laurionite $Pb(OH)Cl$) as secondary corrosion products, and siliceous deposits. The EDX analysis of the internal material (area-b in the SEM image) shows the presence of arsenic and antimony as minor constituents rather related with the ore.

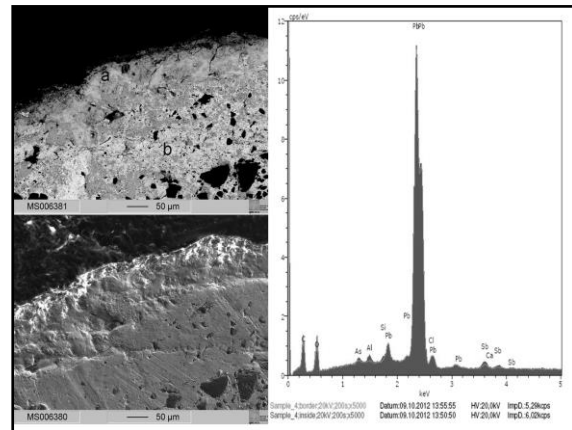


Figure 7: Backscattered (up) and secondary (down) electron SEM images of the the cubic lead weight and corresponding EDX elemental analysis of corrosion (light line) and internal metal (dark line)

The SEM image of the cylindrical lead weight shows a very thin corrosion layer above the internal alloy (Fig. 8). The EDX analysis shows that the corrosion layer (area-a in the SEM image) contains lead, arsenic, antimony, oxygen, carbon, chlorine and silicon. This suggests that the surface of the artifact is covered with lead chloride (cotunnite $PbCl_2$) and/or lead carbonate chloride (phosgenite $Pb_3CO_3Cl_2$) and/or lead chloride hydroxide (laurionite $Pb(OH)Cl$), and siliceous deposits. The EDX analysis of the internal material (area-b in the SEM image) shows the presence of arsenic and antimony as minor constituents. As mentioned previously, these elements would have originated from the ore from which the lead was extracted, and their amounts in the produced lead would vary according to the scheme of smelting process (Gale and Stos-Gale, 1981; Cincotti et al., 2003; Rehren and Prange, 1998).

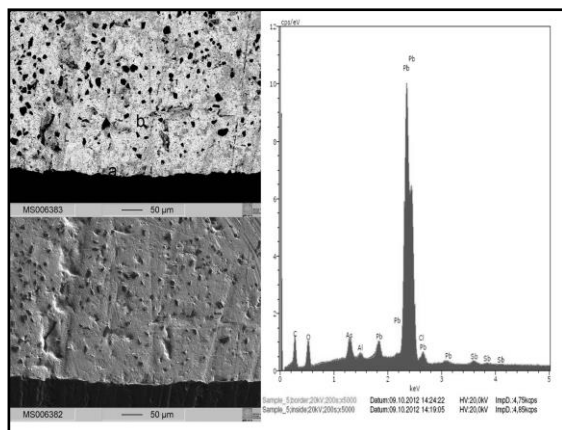


Figure 8: Backscattered (up) and secondary (down) electron Backscattered and secondary electron SEM images of the cylindrical lead weight and corresponding EDX elemental analysis of corrosion (light line) and internal metal (dark line)

The above SEM images of the five lead weights indicate that the corrosion layers, which are mainly composed of lead carbonates, are relatively adherent and protective to the uncorroded metal. However, the presence of the small cracks indicates an intergranular corrosion, which can reduce the ductility and strength of the metal and convert the corrosion product to a powdery material that can easily separate from the surface of the artifact (Mattias, 1984; Nosek, 1985; Turgoose, 1985; Rocca et al., 2004; Alhassan, 2005). In addition, the presence of a mixture of carbonate and chloride based corrosion products indicates a complex corrosion process in the burial soil that contains several anions competing to react with the metal in a series of hydrolysis and precipitation reactions (MacLeod and Wozniak, 1996).

It should be noted that none of the artifacts showed a presence of silver in the EDX analysis. This either indicates the suc-

ACKNOWLEDGEMENTS

This research would have been impossible without the support of the DFG grants; Wassef Sekhaneh gratefully acknowledges the financial support of German Research Society (DFG). All authors would hereby like also to acknowledge Andrea Dellith to her helping for reading this research.

REFERENCES

- Alhassan, S. J. (2005) Corrosion of lead and lead alloys. In *ASM Handbook, Volume 13B: Corrosion: Materials*, S.D. Cramer, B.S. Covino, Jr.(ed.), ASM International, Ohio.

cess of the Romans in desilvering galena by cupellation, or the use of a non-argentiferous galena (PbS) to obtain lead. In addition, the absence of sulfur in the EDX analysis indicates a roasting process at a relatively low temperature in an ample of air supply, thus most of the sulfur was removed as sulfur dioxide gas (Cincotti, 2003).

It is generally approved that lead is produced in the furnace by a double decomposition reaction of its most common ore galena. This involves two consecutive chemical steps (Tylcote, 1962; Davis et al., 1995):

The resulted lead bullion could be remelted for further refining by skimming off the dross layer, and the refined lead is then cast into trade ingots. These ingots would later be used in the manufacture of various lead objects such as the cast lead weights investigated in this study.

7. CONCLUSION

The elemental analysis of the five Roman lead-based scale weights showed that they were cast from a relatively pure lead metal. The surfaces of these artefacts have corroded over the burial and storage years and formed the lead carbonate cerussite as the main corrosion product. Chloride based corrosion products have also formed as secondary products. The formed corrosion products are stable, however slightly cracked and obscuring the surface details. It can be concluded that the artefacts need to be treated to reduce the corroded surface back to compact metal.

- Al-Shiyab, A. M. (2002). *La Jordanie et la Conquête Arabe: 'āb, al-Balqā, al-'Urdunn*. Ph.D. Thesis, Department de Histoire Ancienne et Archeologie, Universite de Versailles Saint-Quentin-en-Yvelines.
- Al-Shiyab, A. M. (1993). Excavation at Al-Qasr and Ar-Rabba, unpublished excavation report at Faculty of archaeology, Yarmouk University in Jordan.
- Bernard, M. Costa, V. and Joiret, S. (2009) Assessing indoor lead corrosion using Raman Spectroscopy during electrochemical reduction. *e-Preservation Science*, vol. 6, 101-106.
- Brooker, M. Sunder, S. Taylor, P. and Lopata, V. (1983) Infrared and Raman spectra and X-ray diffraction studies of solid lead (II) carbonates. *Canadian Journal of Chemistry*, vol. 61, No. 3, 494-502.
- Cagnat, R. (1898) *Cours d'épigraphie Latine*, 3rd edition, Fontemoing, Paris.
- Caley, E. R. (1955) Coatings and incrustations on lead objects from the Agora and the method used for their removal. *Studies in Conservation*, vol. 2, No. 2, 49-54.
- Carradice, I. A. and Campbell, S. A. (1994) The conservation of lead communion tokens by potentiostatic reduction. *Studies in conservation*, vol. 39, No. 2, 100-106.
- Cincotti, A. Massidda, L. and Sanna, U. (2003) Chemical and isotope characterization of lead finds at the Santa Barbara nuraghe (Bauladu, Sardinia). *Journal of Cultural Heritage*, vol. 4, No. 4, 263-268.
- Costa, V. and Urban, F. (2005) Lead and its alloys: metallurgy, deterioration and conservation. *Reviews in Conservation*, No. 6, 48-62.
- Craddock, P.T. (1995) *Early Metal Mining and Production*, Edinburgh University Press, Edinburgh.
- Cronyn, J. (1990) *The elements of archaeological conservation*, Routledge, London.
- Davis, M. Hunter, F. and Livingstone, A. (1995) The corrosion, conservation and analysis of a lead and cannel coal necklace from the early bronze age. *Studies in Conservation*, vol. 40, No. 4, 257-264.
- Gale, N.H. and Stos-Gale, Z.A. (1981) Lead and silver in the ancient Aegean. *Scientific American*, vol. 244, No. 6, 176-192.
- Hultsch, F. (1882) *Griechische und Römische Metrologie*, Weidmann, Berlin.
- Lang, M. and Crosby, M. (1964) *The Athenian Agora, volume X: weights, measures and tokens*, The American School of Classical Studies at Athens, New Jersey.
- MacLeod, I. and Wozniak, R. (1997) Corrosion and conservation of tin and pewter. In *Metal 95: Proceeding of the International Conference on Metals Conservation*, I. MacLeod, L. Robbiola, and S. L. Pennec (eds.), James and James, London.
- Mattias, P Maura, G. and Rinaldi, G. (1984) The degradation of lead antiquities from Italy. *Studies in Conservation*, vol. 29, No. 2, 87-92.
- Meyer, H. and Moreno, A. (2004) A Greek metrological koine: A lead weight from the western Black Sea region in the Ashmolean. *Oxford Journal of Archaeology*, vol. 23, No. 2, 209-216.
- Nriagu, J.O. (1983) *Lead and Lead Poisoning in Antiquity*, John Wiley & Sons, New Jersey.
- Nosek, E. (1985) The investigation and conservation of a lead paten from the eleventh century. *Studies in Conservation*, vol. 30, No. 1, 19-22.
- Pulsifer, W. H. (1888) *Notes for a History of Lead*, University Press, New York.
- Retief, F. and Cilliers, L. (2006) Lead Poisoning in Ancient Rome. *Acta Theologica Supplementum* 7, vol. 26, No. 2, 147-164.
- Rocca, E. Mirambet, F and Steinmetz, J. (2004) Study of ancient lead materials: A gallo-roman sarcophagus – contribution of the electrolytic treatment to its restoration. *Journal of Materials Science*, vol. 39, No. 8, 2767-2774.
- Scott, D. (1996) A note on the metallographic preparation of ancient lead. *Studies in Conservation*, vol. 41, No. 1, 60-62.

- Selwyn, L. (2004) *Metals and corrosion: A handbook for the conservation professional*, Canadian Conservation Institute, Ottawa.
- Turgoose, S. (1985) The corrosion of lead and tin: before and after excavation'. In *Lead and tin: studies in conservation and technology*, G. Miles and S. Pollard (eds), United Kingdom Institute for Conservation, London.
- Tylecote, R. (1962) *Metallurgy in Archaeology*, Edward Arnold Publishers Ltd., London.
- Waterhouse, S. D. (1998) Tomb Type I: Chamber tombs with loculi radiating from the chamber. In *The Necropolis of Hesban: A typology of tombs*, S. D. Waterhouse (ed.), Andrews University Press, Michigan.
- Woolley, D. E. (1984) A perspective of lead poisoning in antiquity and the present. *Neurotoxicology*, vol. 5, No. 3, 353-361.